HIV Protease Inhibitors Block Akt Signaling and Radiosensitize Tumor Cells Both *In vitro* and *In vivo*

Anjali K. Gupta,[1] George J. Cerniglia,[1] Rosemarie Mick,[2] W. Gillies McKenna,[1] and Ruth J. Muschel[3]

Departments of [1]Radiation and [2]Biostatistics and Epidemiology, University of Pennsylvania; [3]Department of Pathology, Children's Hospital of Philadelphia, Philadelphia, Pennsylvania

Abstract

In tumor cells with mutations in epidermal growth factor receptor (SQ20B), H-Ras (T24), or K-Ras (MIAPACA2 and A549), the inhibition of Akt phosphorylation increases radiation sensitivity in clonogenic assays, suggesting that Akt is a potential molecular target when combined with therapeutic radiation. Insulin resistance and diabetes are recognized side effects of HIV protease inhibitors (HPIs), suggesting that these agents may inhibit Akt signaling. Because activation of the phosphatidylinositol 3-kinase (PI3K)-Akt signaling pathway is common in human cancers, we hypothesized that HPIs can inhibit Akt activity resulting in increased tumor cell sensitivity to ionizing radiation–induced cell death. Five first-generation HPIs were subsequently tested and three of the five (amprenavir, nelfinavir, and saquinavir but not ritonavir or indinavir) inhibited Akt phosphorylation at Ser^{473} at serum concentrations routinely achieved in HIV patients. In both tumor cell colony formation assays and tumor regrowth delay experiments, combinations of drug and radiation exerted synergistic effects compared with either modality alone. In addition, *in vivo*, doses of amprenavir or nelfinavir comparable with the therapeutic levels achieved in HIV patients were sufficient to down-regulate phosphorylation of Akt in SQ20B and T24 xenografts. Finally, overexpression of active PI3K in cells without activation of Akt resulted in radiation resistance that could be inhibited with HPIs. Because there is abundant safety data on HPIs accumulated in thousands of HIV patients over the last 5 years, these agents are excellent candidates to be tested as radiation sensitizers in clinical trials. (Cancer Res 2005; 65(18): 8256-65)

Introduction

The tendency of tumor cells to gain resistance to multiple forms of therapy concurrently has long been a barrier to effective treatment, including ionizing radiation (IR) that is used to treat ~60% of all cancer patients in the United States (1). This resistance significantly reduces treatment options and makes disease-free recovery difficult (2, 3). Therefore, the ability to discern particular mechanisms governing multimodality tumor cell resistance and subsequently exploit them should result in more effective treatment strategies.

One such factor known to increase cellular resistance to radiation is the presence of overexpressed or activated oncogenes, such as epidermal growth factor receptor (EGFR; refs. 4–6) and Ras (7, 8), or loss of the tumor suppressor gene *PTEN* (9). One critical observation is that these mutations share a common molecular signaling alteration that ultimately activates the phosphatidylinositol 3-kinase (PI3K)-Akt pathway. In this regard, we and others have shown that blocking PI3K enhances the radiation response *in vitro* and *in vivo*. This effect occurs in cells in which this pathway is constitutively activated but does not affect cells quiescent in this pathway (10–12). Down-regulation of Akt using small interfering RNA also radiosensitizes these cells (13). Because this pathway is frequently activated in tumor cells but not in the normal host cells, it is an excellent candidate to target to increase radiation sensitivity. The problem has been to identify inhibitors of this pathway suitable for clinical use. For example, LY294002 and wortmannin, which are widely used to inhibit the PI3K pathway *in vitro* with significant radiosensitizing effects, however, are poorly tolerated *in vivo* and of little clinical value (14).

In this study, we explore the possibility that one class of drugs in common use clinically, the HIV protease inhibitors (HPIs), may interfere with PI3K-Akt signaling. These drugs given in combination with reverse transcriptase inhibitors are the mainstays of the current therapeutic regimens for HIV-infected patients. The HPIs are peptidomimetics that inhibit the HIV aspartyl protease, a retroviral enzyme that cleaves the viral gag-pol polyprotein and is necessary for the production of infectious viral particles (15). A prominent side effect of HPI treatment is insulin resistance and diabetes (16, 17). Because Akt, especially the Akt2 isoform (18), plays a key role in the coordinated regulation of growth and metabolism by the insulin/insulin-like growth factor signaling pathway (18, 19), we explored the possibility that HPIs might block the PI3K-Akt signaling axis in tumor cells and hence be used clinically as radiation sensitizers. In fact, Pajonk et al. have shown that one HPI, saquinavir, was a radiation sensitizer in tissue culture (20). Here, we found that three of the five HPIs that we tested were able to inhibit Akt at doses routinely achieved clinically. These compounds also sensitized tumor cells both *in vitro* and *in vivo* to radiation. HPIs have been used continuously in patients with well-characterized pharmacokinetics. They are well tolerated; thus, testing these HPIs as radiation sensitizers could easily proceed to clinical trial.

Materials and Methods

Cells. SQ20B, T24, MIAPACA2, and A549 cell lines were obtained from American Type Culture Collection (Rockville, MD). The MR4 cells were derived from isogenic rat embryo fibroblasts by transfection with v-*myc* as described previously (8). Cells were cultured in DMEM (Fisher Scientific, Pittsburgh, PA) supplemented with 10% fetal bovine serum (Atlanta Biologicals, Norcross, GA), penicillin (100 units/mL), and streptomycin (100 mg/mL; Life Technologies, Gaithersburg, MD) at 37°C in humidified 5% CO_2/95% air.

Requests for reprints: Anjali K. Gupta, Department of Radiation Oncology, University of Pennsylvania, 195 JMB, 3620 Hamilton Walk, Philadelphia, PA 19104. Phone: 215-898-0076; Fax: 215-898-0996; E-mail: gupta@xrt.upenn.edu.

doi:10.1158/0008-5472.CAN-05-1220

Table 1. Surviving fraction after 2 Gy (SF2) in cell lines ± HPIs

Cell line	Cancer type	Mutation	Control SF2, *n* (mean ± SD)	Amprenavir SF2, *n* (mean ± SD) [*P*]	Nelfinavir SF2, *n* (mean ± SD) [*P*]
T24	Bladder	H-Ras	6 (0.560 ± 0.061)	6 (0.370 ± 0.022) [<0.001*]	6 (0.452 ± 0.023) [0.006*]
SQ20B	Head and neck	EGFR	6 (0.691 ± 0.042)	6 (0.432 ± 0.017) [<0.001*]	5 (0.401 ± 0.024) [<0.001*]
MIAPACA2	Pancreatic	K-Ras	4 (0.906 ± 0.086)	5 (0.664 ± 0.051) [0.001*]	5 (0.526 ± 0.040) [0.001*]
A549	Lung	K-Ras	6 (0.570 ± 0.042)	5 (0.487 ± 0.030) [0.002*]	4 (0.401 ± 0.062) [<0.001*]
REF	Rat fibroblasts	None	5 (0.408 ± 0.040)	4 (0.402 ± 0.136) [0.89*]	5 (0.397 ± 0.054) [0.89*]

*Compared with control SF2 by *t* test.

MR4 cells were transfected with constitutively active PI3K consisting of the iSH2 domain of p85 fused to the NH_2 terminus of p110 by means of a flexible glycine linker (21) inserted into the pGRE5/EBV dexamethasone-inducible plasmid vector. Because this is an episomal vector, a pool of cells was selected with hygromycin for 72 hours. Dexamethasone (Sigma, St. Louis, MO) at 1 μg/mL was added. Radiation survival experiments were done and protein samples were harvested 24 hours after the addition of dexamethasone.

Drugs. The HPIs were bought for research use from the hospital inpatient pharmacy of the University of Pennsylvania. Ritonavir, amprenavir, and saquinavir came as gelatin capsules. The capsule was punctured and the viscous liquid inside was dissolved in 100% ethanol to make a concentrated stock solution for subsequent experiments. Nelfinavir and indinavir came as solid caplets and were ground into a fine powder and subsequently dissolved in 100% ethanol.

Western blotting. Cells were lysed without trypsinization by rinsing culture dishes once with PBS followed by lysis with reducing Laemmli sample buffer. Samples were boiled, sheared, clarified by centrifugation, and stored at −20°C. Samples containing equal amounts of protein were separated on a 12% SDS-polyacrylamide gel and blotted onto nitrocellulose membranes. Membranes were blocked in PBS containing 0.1% Tween 20 and 5% powdered milk before primary antibody addition. Both polyclonal anti-phospho-Ser^{473} Akt and total Akt antibodies (New England Biolabs, Ipswich, MA) were used at a dilution of 1:2,000. Polyclonal anti–mitogen-activated protein kinase (MAPK) K-23 antibody (Santa Cruz Biotechnology) was used at a dilution of 1:500. Monoclonal anti-β-actin antibody (Sigma) was used at a dilution of 1:4,000. Antibody binding was detected using the enhanced chemiluminescence kit (Amersham, Arlington Heights, IL). Images were digitized using an Arcus II scanner, and figures were assembled using Adobe Photoshop 3.0 and Microsoft Power Point.

Radiation survival determination. Cells in exponential growth phase were counted and plated in 60-mm dishes containing 4 mL medium. The cells were allowed to attach and drugs were added to cultures at least 1 hour before radiation. Cells were irradiated with a Mark I cesium irradiator (J.L. Shepherd, San Fernando, CA) at a dose rate of 1.6 Gy/min. Colonies were stained and counted 10 to 14 days after irradiation. A colony by definition had >50 cells. The surviving fraction was calculated by dividing the number of colonies formed by the number of cells plated times plating efficiency. Each point on the survival curve represents the mean surviving fraction from at least three replicates.

Cell growth curves. Cells (3×10^5) were plated in each T25 flask. The cells were allowed to attach and enter exponential growth and the drugs were added. At various times, total cell number was assessed in triplicate.

Tumor generation in nude mice. Pathogen-free female Ncr-*nu/nu* mice were obtained from Taconic (Germantown, NY) and housed aseptically in the animal facilities of University Laboratory Animal Resources and the Institute for Human Gene Therapy of the University of Pennsylvania. All experiments were carried out in accordance with University Institutional Animal Care and Use Committee guidelines. At 5 to 7 weeks of age, mice were inoculated by s.c. injection into the hind flank with 1×10^7 T24 or 1×10^6 SQ20B cells resuspended in 100 μL Matrigel (BD Collaborative Research, Franklin Lakes, NJ). SQ20B tumors usually appeared within 1 week and T24 tumors 2 to 3 weeks after injection.

Drug treatment of mice. Nelfinavir was formulated as 3-week continuous release pellets containing 12.6 mg drug with a release rate of 0.6 mg/d by Innovative Research of America (Sarasota, FL). Amprenavir was given s.c. by continuous micro-osmotic pump infusion (Alza Corp.,

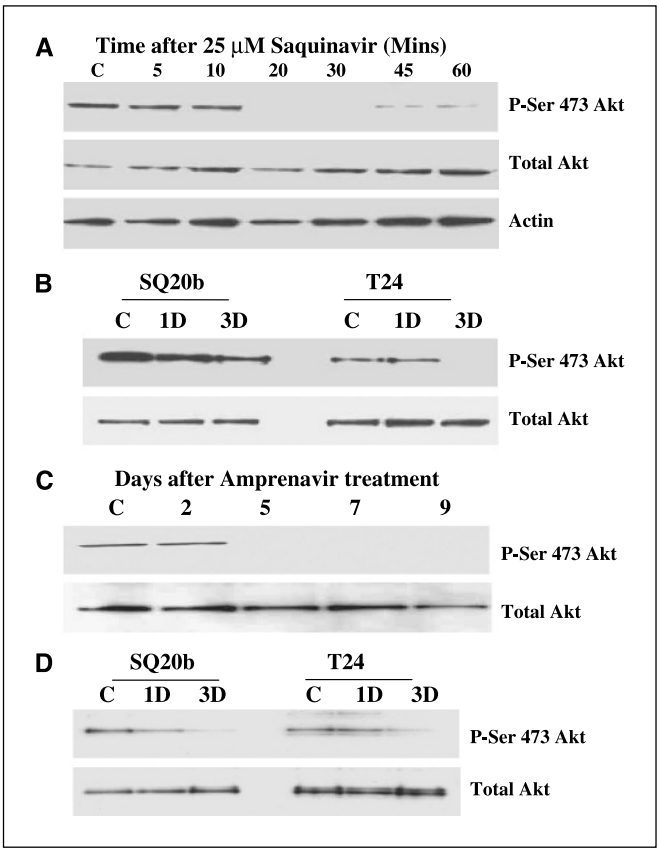

Figure 1. Effect of HPIs on phosphorylation of Akt, MAPK, and p70S6K. SQ20B or T24 cells in tissue culture were treated with the indicated HPIs. At the indicated times, cells were harvested and immunoblotted with antibody used to detect the active or phosphorylated forms of Ser^{473} Akt, Thr^{308} Akt, MAPK, or p70S6K. Antibodies detecting total Akt, MAPK, and actin were also used. *A,* SQ20B cells were treated with 25 μmol/L saquinavir from 5 to 60 minutes. *B,* SQ20B or T24 cells were treated with 5 μmol/L amprenavir for 1 or 3 days. *C,* SQ20B cells were treated with 10 μmol/L amprenavir for 2, 5, 7, or 9 days. *D,* SQ20B or T24 cells were treated with 5 μmol/L nelfinavir for 1 or 3 days.

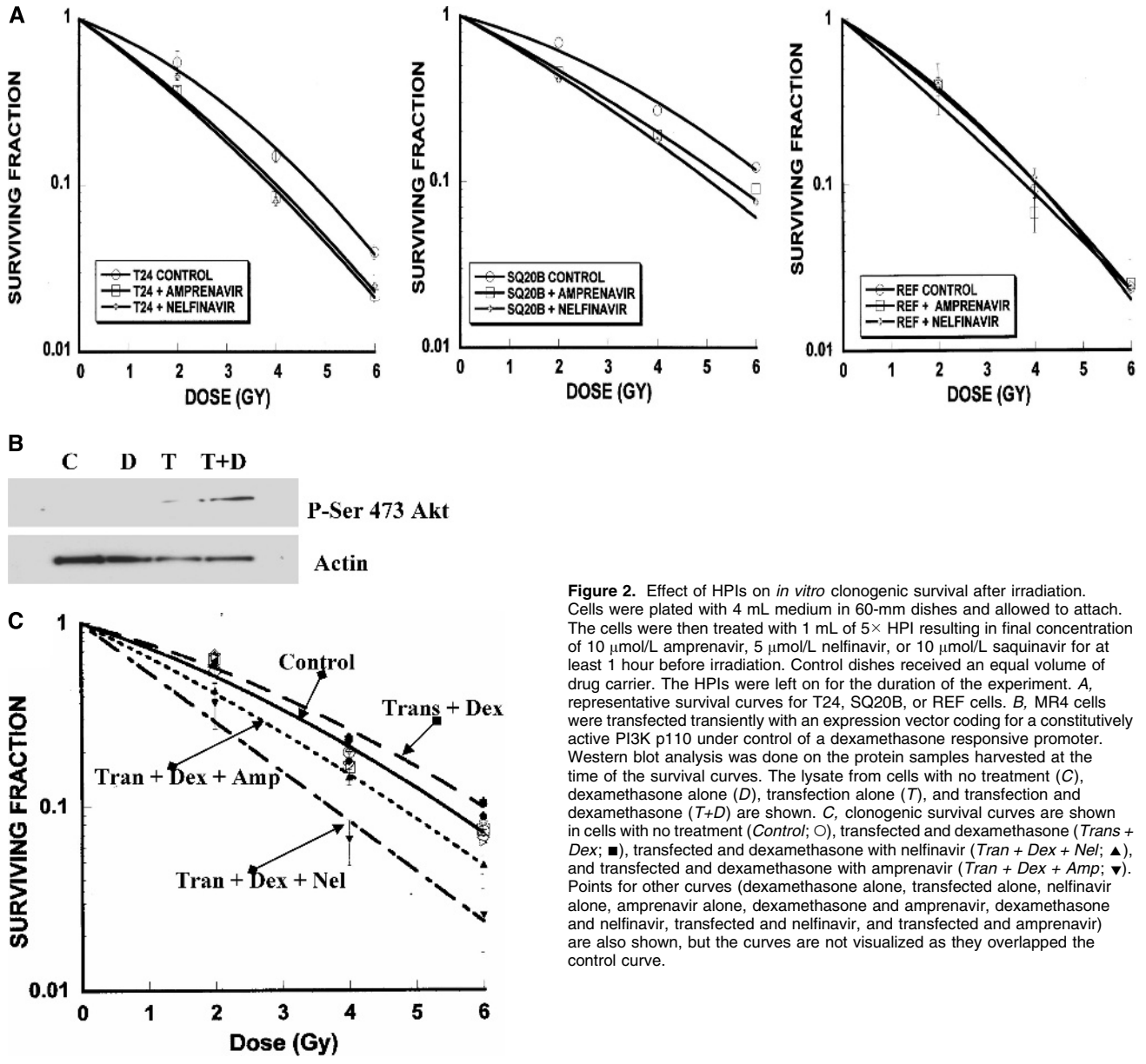

Figure 2. Effect of HPIs on *in vitro* clonogenic survival after irradiation. Cells were plated with 4 mL medium in 60-mm dishes and allowed to attach. The cells were then treated with 1 mL of 5× HPI resulting in final concentration of 10 μmol/L amprenavir, 5 μmol/L nelfinavir, or 10 μmol/L saquinavir for at least 1 hour before irradiation. Control dishes received an equal volume of drug carrier. The HPIs were left on for the duration of the experiment. *A,* representative survival curves for T24, SQ20B, or REF cells. *B,* MR4 cells were transfected transiently with an expression vector coding for a constitutively active PI3K p110 under control of a dexamethasone responsive promoter. Western blot analysis was done on the protein samples harvested at the time of the survival curves. The lysate from cells with no treatment (*C*), dexamethasone alone (*D*), transfection alone (*T*), and transfection and dexamethasone (*T+D*) are shown. *C,* clonogenic survival curves are shown in cells with no treatment (*Control*; ○), transfected and dexamethasone (*Trans + Dex*; ■), transfected and dexamethasone with nelfinavir (*Tran + Dex + Nel*; ▲), and transfected and dexamethasone with amprenavir (*Tran + Dex + Amp*; ▼). Points for other curves (dexamethasone alone, transfected alone, nelfinavir alone, amprenavir alone, dexamethasone and amprenavir, dexamethasone and nelfinavir, transfected and nelfinavir, and transfected and amprenavir) are also shown, but the curves are not visualized as they overlapped the control curve.

Palo Alto, CA) of the drug at a dose of 0.8 mg/d. These doses are comparable with that used in HIV patients. Control animals received placebo pellet or pumps with carrier alone.

Drug measurements in serum. High-performance liquid chromatography was done using a binary gradient Jasco system. Serum was prepared by adding an equal part of 100% methanol followed by incubation on ice for 1 hour and centrifugation at 13,000 × *g* for 10 minutes. The supernatant (100 μL) was analyzed using an Alltima C18 column (4.6 × 250 mm, 5 μ) with buffer [0.1 mmol/L ammonium acetate (pH 4.7)] gradient for nelfinavir of 30% to 90% (4 minutes) followed by 90% (8 minutes) and for amprenavir of 30% to 90% (10 minutes) followed by 90% (4 minutes). Nelfinavir or amprenavir content was determined from the area under curve at the drug peak detected at 11 to 12 minutes with λ260 for amprenavir and λ250 for nelfinavir. Absolute values were calculated from calibration curves.

Immunohistochemical staining. Paraffin-embedded tissue sections were stained with antibody for immunohistochemistry to phospho-Ser^{473} Akt as described by Zhou et al. (22). Slides were graded as 0 to 3+ staining as we have described previously (12).

***In vivo* clonogenic assays.** Animals were assigned randomly to treatment groups (control, radiation alone, drug alone, or radiation and drug) when tumors attained a volume of 300 to 400 mm^3. Drug treatment was started 3 days (amprenavir) or 5 days (nelfinavir) before radiation. Mice were irradiated with doses of 6 to 8 Gy with a Mark I cesium irradiator at a dose rate of 1.6 Gy/min under anesthesia. Unirradiated animals were anesthetized and sham irradiated. One hour after irradiation, animals were sacrificed. Tumors were then excised, minced, and dissociated for 30 minutes at 37°C in HBSS containing 166 units/mL collagenase XI, 0.25 mg/mL protease, and 255 units/mL DNase. Cells were recovered after straining through an 80-μm mesh. The cells were pelleted by centrifugation at 500 × *g* and resuspended in culture medium. Cells were counted by hemocytometer using trypan blue to determine viability, and the counts were verified by Coulter counter analysis. Cells were then plated in 100-mm dishes and cultured for 14 to

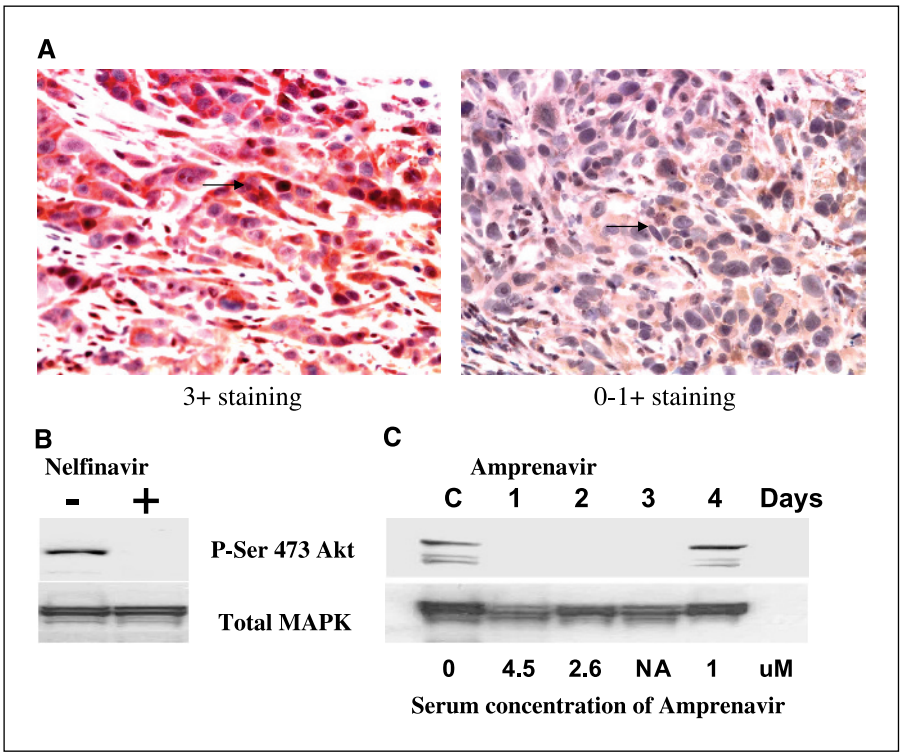

Figure 3. *In vivo* down-regulation of phosphorylated Ser^{473} Akt in xenografts with amprenavir or nelfinavir. *A,* immunohistochemistry (400×) of representative SQ20B tumor from a control mouse (*left*) and a mouse treated with nelfinavir (*right*). The tumors were harvested 5 days after being treated with placebo or nelfinavir 0.6 mg/d. *B,* an immunoblot of the lysate from the tumors shown in *A*. *C,* an immunoblot of the lysates from SQ20B tumors treated with amprenavir 0.8 mg/d for 1, 2, 3, or 4 days. The serum concentration of amprenavir corresponding to the treatment is shown below the blot.

21 days, after which colonies were stained and counted. Results are expressed as the plating efficiency determined from replicate dishes plated at multiple initial cell densities.

Determinations of tumor regrowth delay. Mice bearing established tumors were randomized and treated with amprenavir/nelfinavir as described above. Irradiation (6 or 8 Gy) of the flank bearing the tumor was done using a 250 kV orthovoltage irradiator (Philips RT 250) at a dose rate of 2.63 Gy/min through a 0.2-mm copper filter. The source-to-tumor target distance was 30 cm with adequate shielding of nontumor sites. Mice were examined twice weekly for evaluation of tumor growth. Tumors were measured with calipers in three mutually perpendicular diameters (a, b, and c) and the volume was calculated as $V = (\pi / 6) \times a \times b \times c$.

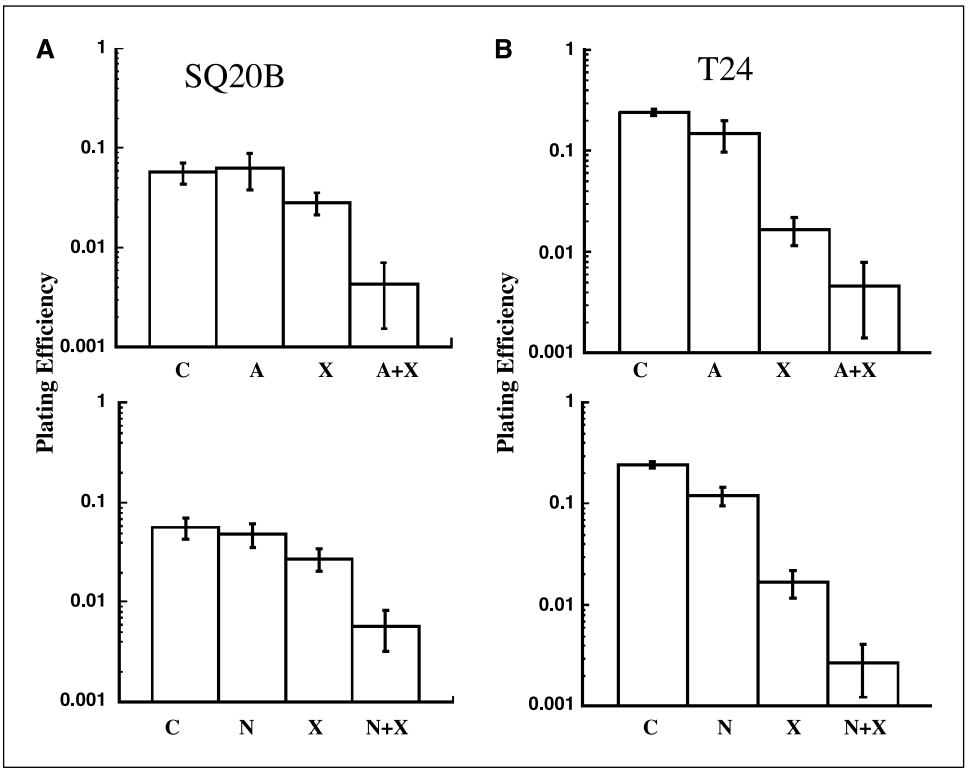

Figure 4. Effect of HPIs on the tumor *in vivo* clonogenicity after radiation. *A,* effect of amprenavir (*A*) or nelfinavir (*N*) on the *in vivo* clonogenicity of SQ20B xenografts. *X,* treatment with 8 Gy radiation. *B,* same as *A*, except for in T24 xenografts. *X,* treatment with 6 Gy radiation.

Table 2. Test of synergy in SQ20B xenografts for *in vivo* to *in vitro* clonogenicity with radiation and amprenavir or radiation and nelfinavir

Log_{10} plating efficiency mean* ± SD (no. measures per mouse)

Control (n = 4)	8 Gy (n = 5)	Amprenavir (n = 5)	8 Gy + Amprenavir (n = 4)	Nelfinavir (n = 3)	8 Gy + Nelfinavir (n = 4)
−1.24 ± 0.06 (8-12)	−1.54 ± 0.09 (8-12)	−1.21 ± 0.13 (8-12)	−2.37 ± 0.25 (6-12)	−1.29 ± 0.05 (4-6)	−2.30 ± 0.24 (6-7)

Interaction term β (SE)	−0.864 (0.138)	−0.707 (0.137)
Wald statistic	−6.283	−5.153
Test of synergy (one-sided P)	<0.001	<0.001

*Mean of the averages for each mouse.

Statistical analysis. A two-sided Student's t test was used to determine significance between SF2s in Table 1. A regression model was fit to log_{10}-transformed plating efficiency data that included terms to estimate the individual (main) effects of radiation and HPI and the interaction of these two treatments on the mean plating efficiency of tumor cells. Replicate measurements were averaged for each mouse. The linear model took the form:

$$Y = \beta_0 + \beta_1(\text{radiation}) + \beta_2(\text{HPI}) + \beta_3(\text{radiation} \times \text{HPI}),$$

where $Y = \log_{10}$ plating efficiency, radiation, and HPI are indicators for the treatment received (1 = yes, 0 = no) and radiation × HPI is an interaction term. The test of synergy between radiation and HPI was conducted on the interaction term using a one-sided Wald statistic to determine whether $\beta_3 < 0$, indicating synergy. A negative coefficient for the interaction term indicates a synergistic effect and a more than additive decrease in plating efficiency. $P = 0.05$ was considered to be significant. Time to tumor volume of 1,000 mm^3 was analyzed in a similar manner, with Y equal to days to reach a volume of 1,000 mm^3 during the observation period. The test of synergy between radiation and HPI was again conducted on the interaction term using a one-sided Wald statistic. For regrowth studies, $\beta_3 > 0$ indicates synergy and a more than additive increase in time to tumor volume of 1,000 mm^3. In T24 tumors, a single mouse in both radiation plus amprenavir and radiation plus nelfinavir treatment group did not reach a volume of 1,000 mm^3 during the observation period. All observations in the radiation plus amprenavir group and all but one in the radiation plus nelfinavir group exceeded those of the control and single modality groups, which resulted in either singularity and/or failure of a Cox regression model to converge. Thus, each censored was treated as an event on day 35 and linear regression was then employed to test synergy. This approach produces a slightly conservative estimate of treatment effect for the data described above. All analyses were done in SPSS 12.0 (SPSS, Inc., Chicago, IL).

Results

Inhibition of Akt signaling by HIV protease inhibitors in tissue culture. Insulin resistance and diabetes are well-established and recognized side effects of extended HPI use, and it has been suggested that this may be due to inhibition of Akt signaling. Because Akt activity is involved in tumor cell resistance, it seemed logical to determine if HPIs may inhibit Akt. Between 1995 and 1999, five HPIs were approved by the Food and Drug Administration: saquinavir, ritonavir, indinavir, nelfinavir, and amprenavir. We tested these drugs for their effects on Akt phosphorylation. Two cell lines with constitutively active Akt signaling phosphorylation of Akt Ser^{473} were initially chosen: (*a*) SQ20B cells with overexpression of activated EGFR and (*b*) T24 cells that contain an oncogenic mutation in H-Ras and an allelic amplification of that allele. Complete Akt activation requires phosphorylation of Ser^{473}.

SQ20B cells were treated with 25 μmol/L saquinavir from 5 to 60 minutes and Western blot analysis showed a time-dependent decrease in immunoreactive Akt phosphorylation levels with a complete loss of detectable phosphorylation of Akt within 20 minutes (Fig. 1*A*). There was no change in the total Akt levels using actin as a loading control. At lower concentrations (5-10 μmol/L

Table 3. Test of synergy in T24 xenografts for *in vivo* to *in vitro* clonogenicity with radiation and amprenavir or radiation and nelfinavir

Log_{10} plating efficiency mean* ± SD (no. measures per mouse)

Control (n = 5)	6 Gy (n = 3)	Amprenavir (n = 3)	6 Gy + Amprenavir (n = 4)	Nelfinavir (n = 3)	6 Gy + Nelfinavir (n = 2)
−0.62 ± 0.03 (12)	−1.80 ± 0.15 (12)	−0.85 ± 0.17 (12)	−2.45 ± 0.39 (11-12)	−0.93 ± 0.09 (12)	−2.60 ± 0.25 (12)

Interaction term β (SE)	−0.420 (0.239)	−0.499 (0.138)
Wald statistic	−1.760	−3.621
Test of synergy (one-sided P)	0.053	0.003

*Mean of the averages for each mouse.

range), saquinavir took ~24 hours to have the same effect (data not shown). However, saquinavir was highly toxic in tissue culture with cell death within 2 hours of treatment at 25 μmol/L and cell death at 24 to 48 hours for doses between 1 and 10 μmol/L.

Treatment of SQ20B cells with amprenavir (5 μmol/L) resulted in down-regulated phosphorylation of Akt at Ser^{473} after a 3-day exposure (Fig. 1*B*) with no effect on total intracellular Akt levels. In addition, treatment of SQ20B cells with amprenavir (10 μmol/L) also resulted in complete dephosphorylation of Akt at Ser^{473} and this was observed for at least 9 days (Fig. 1*C*). Exposure to higher doses of amprenavir (20-25 μmol/L) resulted in more rapid down-regulation of Akt at 1 day but not sooner than 16 hours. Finally, at amprenavir concentrations that inhibited Akt phosphorylation (5-10 μmol/L), no effect on cell growth was observed (data not shown). However, at higher doses (40 μmol/L) or longer exposures (>16 hours), significant tumor cell toxicity was observed, suggesting that inhibition of Akt activity has little effect on cell death at these clinically achievable concentrations.

Similar to saquinavir and amprenavir, nelfinavir (5 μmol/L) down-regulated Akt phosphorylation at Ser^{473} in both SQ20B and T24 cells (Fig. 1*D*) without change in total intracellular Akt protein levels. Exposure to increasing the concentration of nelfinavir resulted in an earlier onset of this response but resulted in cell toxicity at 20 μmol/L. Finally, similar to the other HPIs tested, no changes in cell growth kinetics or cell death was observed at concentrations that inhibit Akt phosphorylation (data not shown).

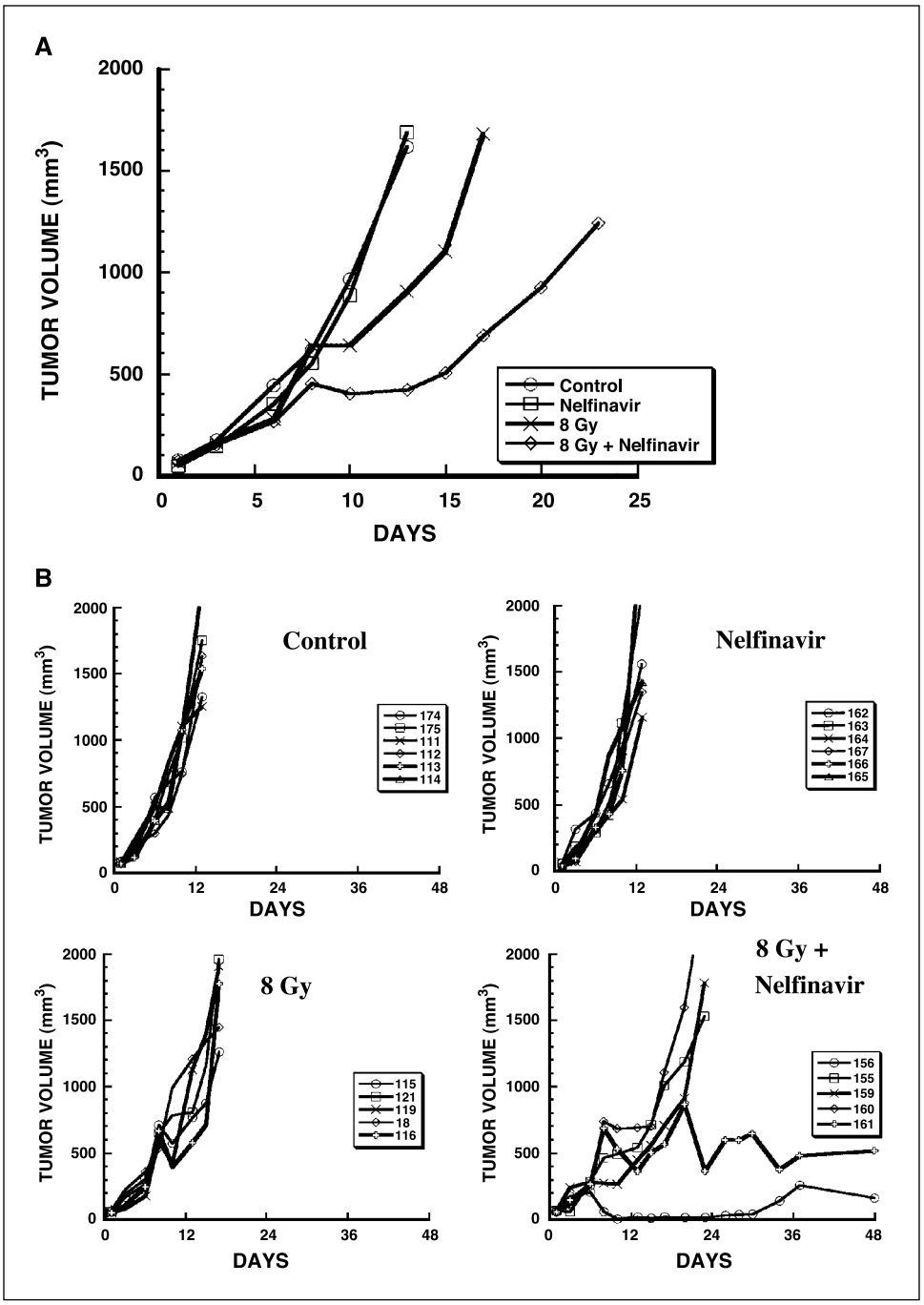

Figure 5. Regrowth delay of SQ20B xenografts ± nelfinavir after radiation. *A,* mean tumor volume in control tumors (○), nelfinavir-treated tumors (□), tumors treated with 8 Gy radiation (×), or 8 Gy and nelfinavir-treated tumors (◇). *B,* data from each individual tumor, which were used to derive the data in *A*.

Table 4. Test of synergy for regrowth delay in time to reach tumor volume of 1,000 mm^3 in SQ20B xenografts ± nelfinavir after radiation

Days to tumor volume of 1,000 mm^3 mean ± SD (range)			
Control (n = 6)	Nelfinavir (n = 6)	8 Gy (n = 5)	8 Gy + Nelfinavir (n = 5)
11.0 ± 1.5 (10-13)	12.0 ± 1.5 (10-13)	15.0 ± 2.0 (13-17)	41.0 ± 30.3 (17-78)
Interaction term β (SE)		25.000 (12.321)	
Wald statistic		2.029	
Test of synergy (one-sided P)		0.03	

NOTE: All animals reached tumor volume of 1,000 mm^3 before sacrifice.

The other HPIs tested, indinavir and ritonavir, did not appreciably affect cell growth, toxicity, or regulation of Akt signaling at concentrations up to 100 μmol/L (data not shown).

Radiation sensitization by HIV protease inhibitors *in vitro*. We have shown previously that inhibition of the PI3K-Akt pathway increases radiosensitivity of tumor cells (11). Insulin resistance and diabetes are recognized side effects of HPIs, suggesting that these agents may inhibit of Akt signaling. Because activation of the PI3K-Akt signaling pathway seems to confer resistance to IR-induced cell death, it seemed logical to hypothesize that HPIs can inhibit Akt activity resulting in increased tumor cell sensitivity to IR-induced cell death. To address this idea, two cell lines were tested, SQ20B and T24, which contain constitutively active Akt, as determined by increased Akt phosphorylation. Experiments were subsequently expanded to include two additional cell lines, MIAPACA2 (pancreatic tumor cells) and A549 (lung tumor cells), both of which contain an activating K-Ras mutation. Initially, clonogenic cell survival experiments were done to determine any changes in radiosensitivity *in vitro*. Results from these experiments showed that both T24 and SQ20B cells were sensitized to the cytotoxicity of IR following exposure to either amprenavir (10 μmol/L) or nelfinavir (5 μmol/L; Fig. 2*A*). The SF2 results from these survival experiments are shown (Table 1). Cell survival experiments with saquinavir were limited due to its toxicity, however; exposure of T24 cells inhibited Akt and resulted in radiosensitization. REF cells, which do not have increased Akt phosphorylation and showed no change in radiation-induced cell death, suggests that normal tissues are not affected by exposure to HPIs. In every cell line with increased signaling through Akt, there was at least 15% reduction in surviving fraction with the drug, and in many cases, the reduction was as large as 40%. These results are significant as there is no overlap in the SEs.

To further determine the role of elevated Akt phosphorylation levels on HPI-induced radiosensitization, we transfected MR4 cells expressing wild-type Ras with a constitutively active PI3K under control of a dexamethasone-inducible promoter. The catalytic subunit of PI3K, p110, exhibits enzymatic activity when bound through its NH_2-terminal region to the p85 subunit (23), which allows the construction of a constitutively active PI3K consisting of the iSH2 region of p85 covalently attached to the NH_2 terminus of the p110 subunit (21). Dexamethasone treatment of these transiently transfected cells resulted in the appearance of phosphorylated Akt (Fig. 2*B*). The presence of phosphorylated Akt as a marker for PI3K activity was specific for cells expressing the activated p110 subunit because neither untransfected cells treated with dexamethasone nor uninduced transfectants showed enhanced Akt phosphorylation.

MR4 cells transfected with active PI3K treated with dexamethasone showed a significant increase in resistance to IR-induced cell death, whereas no change in clonogenic cell survival was seen in control cells. Expression of the vector alone and exposure to dexamethasone did not alter the plating efficiency of the cells. In addition, treatment of transfected cells with amprenavir and nelfinavir in the presence of dexamethasone sensitized them to radiation (Fig. 2*C*).

HIV protease inhibitors inhibit Akt signaling *in vivo*. Although *in vitro* data provide an important preliminary background to advance the potential use of new anticancer agents, these results must be confirmed and validated in an *in vivo* tumor model system. Before regrowth experiments, we initially determined if nelfinavir and amprenavir can down-regulate Akt in xenografts. As such, nelfinavir was given at 0.6 mg/d via a continuous releasing pellet and it was observed that a minimum of 5 days of exposure was necessary for serum levels of nelfinavir to equilibrate in the 2 to 6 μmol/L range. The tumors were stained with anti-phospho-Ser^{473} Akt antibody and the phosphorylation was down-regulated from 3+ to 0-1+ staining. Figure 3*A* shows representative sections from SQ20B xenografts, one from a mouse treated with nelfinavir (*right*) and one without (*left*). The serum level of nelfinavir in the mouse treated with drug was 4.5 μmol/L (Fig. 3*B*) and Western blotting with anti-phospho-Ser^{473} Akt confirms the decrease in phospho-Akt seen in tumor slides.

Amprenavir was delivered via micro-osmotic pump at 0.8 mg/d. At this dose, the serum concentrations of the drug were in the 1 to 5 μmol/L range, and 2 to 5 μmol/L were sufficient to down-regulate phosphorylation of Akt at Ser^{473} (Fig. 3*C*). Thus, both amprenavir and nelfinavir down-regulated phosphorylation of Akt at Ser^{473} in tumors *in vivo* at doses comparable with the therapeutic levels achieved in HIV patients.

Radiation sensitization *in vivo* measured by clonogenic assay. Tumor cell colony formation assays were used to measure radiation response after amprenavir and nelfinavir treatment of SQ20B or T24 tumor-bearing animals. The clonogenicity of tumor cells was compared after isolation from tumors treated with radiation plus amprenavir/nelfinavir, radiation alone, amprenavir/nelfinavir alone, or mock treatment. The radiation dose was 8 Gy for SQ20B tumors and 6 Gy for T24 tumors. The animals were pretreated with nelfinavir pellets for 5 days or with amprenavir pumps for 2 days. Both amprenavir and nelfinavir treatment of

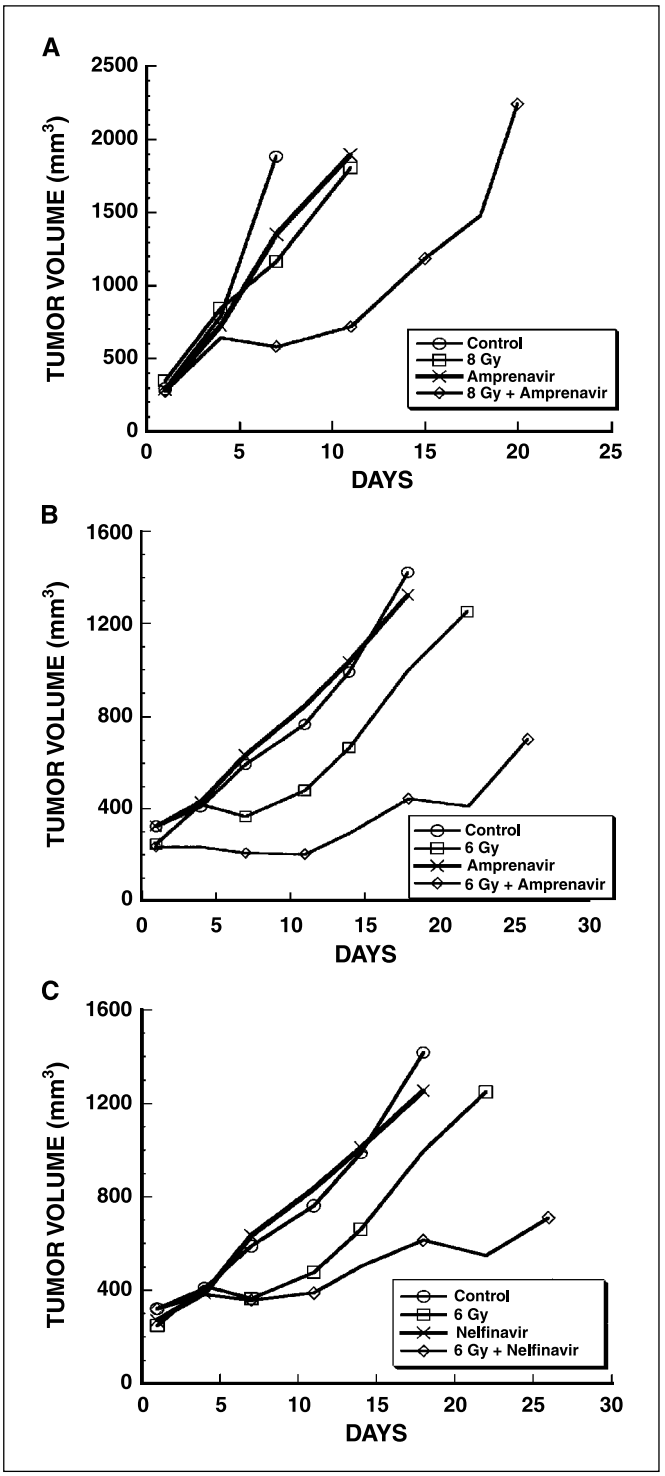

Figure 6. Regrowth delay in SQ20B or T24 xenografts with amprenavir or nelfinavir. The mean tumor volumes in control tumors (○), radiated tumors (□), drug-treated tumors (×), or tumors treated with radiation and drug (◇) are shown. *A,* SQ20B xenografts ± amprenavir. The radiation is 8 Gy. *B,* T24 xenografts ± amprenavir. *C,* T24 xenografts ± nelfinavir. The radiation for the T24 xenografts is 6 Gy.

SQ20B (Fig. 4*A*) or T24 (Fig. 4*B*) xenografts resulted in reduction in clonogenicity after irradiation. As seen in Table 2, both amprenavir and radiation and nelfinavir and radiation in SQ20B xenografts exhibited highly statistically significant synergy ($P < 0.001$ each). In T24 xenografts (Table 3), nelfinavir and radiation exhibited highly statistically significant synergy ($P = 0.003$) and the synergistic effect of amprenavir and radiation nearly reached statistical significance ($P = 0.053$).

HIV protease inhibitors inhibit xenograft tumor regrowth following irradiation. Radiation sensitization was also assessed using the tumor regrowth delay assay. Mice bearing SQ20B or T24 tumors were randomly assigned to each treatment arm (radiation plus drug, radiation alone, drug alone, or mock treatment). As with the clonogenic assays, mice were pretreated for 2 days with amprenavir pumps or 5 days with nelfinavir pellets. The radiation dose was 8 Gy for SQ20B tumors and 6 Gy for T24 tumors. The radiation dose was chosen based to yield a growth delay and not a cure to allow better statistical analysis.

SQ20B tumor xenografts treated with nelfinavir and the results for mean tumor volumes (Fig. 5*A*) and each individual tumors (Fig. 5*B*) are shown. In the radiation plus nelfinavir group, two slowly growing tumors reached a volume of 1,000 mm^3 at 70 and 78 days (data not shown in Fig. 5*B*). The mean time to tumor volume of 1,000 mm^3 was 11 days in the control group and 12 days in the nelfinavir alone group. As expected, mean values increased in both radiation alone (15 days) and radiation and nelfinavir (41 days) groups. As seen in Table 4, a statistically significant synergistic effect between radiation and nelfinavir was detected by linear regression analysis ($P = 0.03$).

In SQ20B xenografts treated with amprenavir, a mean time to tumor volume of 1,000 mm^3 was 5.8 days in the control group (Fig. 6*A*) and 7.1 days in the amprenavir alone group. Mean values increased in both radiation alone (8 days) and radiation and amprenavir (15.8 days) groups. By linear regression analysis, a statistically significant synergistic effect between radiation and amprenavir was detected ($P = 0.0045$; Table 5). Of note is that these tumors were larger at the start of the experiment than the SQ20B tumors with nelfinavir as shown in Fig. 5 (mean starting volume of 300 versus 100 mm^3); thus, the time to reach 1,000 mm^3 was shorter.

In T24 tumors treated with amprenavir (Fig. 6*B*), mean time to tumor volume of 1,000 mm^3 was 15.8 days in the control group, 13.2 days in the amprenavir alone group, and 14.3 days in the nelfinavir alone group. Mean values increased to 19.3 days with 6 Gy radiation alone and 30.8 days with radiation and amprenavir. In contrast, in T24 tumors treated with nelfinavir, mean value was 28.6 days with radiation, which was statistically identical to that of mice treated with amprenavir. Statistically significant synergy was apparent for both radiation and amprenavir ($P < 0.001$; Table 6) and radiation and nelfinavir ($P = 0.004$; Table 7).

We evaluated six mice for normal tissue toxicity from HPI and radiation: two untreated, two treated with nelfinavir, and two treated with amprenavir. The right leg of each mouse was irradiated with 8 Gy. We assessed the mice weekly for the visual development of skin fibrosis and leg contractures. No difference was seen in unirradiated versus irradiated or drug and irradiated legs. At 60 days, the mice were sacrificed and histologic sections of legs were compared. There was an increase in epidermal thickness with irradiation (mean control, 16 versus 22 μmol/L for 8 Gy). It was, however, impossible to tell which mouse had been given the drug versus control and no additive effect on skin fibrosis was seen with HPI and radiation.

Discussion

The PI3K-Akt pathway is frequently constitutively activated in human tumor cells versus normal cells, suggesting that factors in this cascade are potential molecular targets (reviewed in ref. 24). We and others have shown that activation of this pathway results in

Table 5. Test of synergy for regrowth delay in time to reach tumor volume of 1,000 mm^3 in SQ20B xenografts ± amprenavir after radiation

Days to tumor volume of 1,000 mm^3 mean ± SD (range)			
Control (n = 5)	Amprenavir (n = 7)	8 Gy (n = 5)	8 Gy + Amprenavir (n = 5)
5.8 ± 1.6 (4-7)	7.1 ± 2.0 (4-11)	8.0 ± 3.0 (4-11)	15.8 ± 3.4 (11-20)
Interaction term β (SE)		6.457 (2.211)	
Wald statistic		2.920	
Test of synergy (one-sided P)		0.0045	

NOTE: All animals reached tumor volume of 1,000 mm^3 before sacrifice.

resistance to IR in tumor cells in both tissue culture and tumor xenografts *in vivo* (10–12, 14). Because this pathway is not active in most normal tissues, strategies to block PI3K-Akt signaling should result in more effective radiation treatment by enhancing tumor cells to the cytotoxicity of IR while sparing normal tissues surrounding the tumor. However, a major obstruction in implementing this strategy is the identification of agents that inhibit Akt activity with minimal dose limit toxicities or clinically significant side effects.

Here, we have shown that several HPIs have an unexpected ability to inhibit Akt phosphorylation. Both nelfinavir and amprenavir inhibited phosphorylation of Akt Ser^{473} in both tissue culture and *in vivo* experiments. Concomitantly, these drugs sensitized all four tumor cell lines tested *in vitro*. Because radiation is typically given in 2 Gy doses for at least 30 fractions, even a 15% reduction in surviving fraction (0.57-0.487 in A549 cells with amprenavir) translates into an increase of 2 logs of cell kill (0.57^{30} versus 0.487^{30}) with the addition of the drug. The administration of amprenavir or nelfinavir to mice at levels comparable with those used in HIV patients resulted in sensitization of both T24 and SQ20B xenografts after a single dose of radiation. The effect of these HPIs was synergistic with radiation without increase in normal tissue toxicity as determined using REF clonogenicity or epidermal skin thickness in mice with drug treatment and radiation.

Although the translation research presented here clearly shows the clinical potential for amprenavir, nelfinavir, or saquinavir, the exact mechanism by which these agents interfere with the PI3K-Akt signaling pathway remains unclear. The observation that MR4 cells with transfection of active PI3K were also sensitized by the protease inhibitors leads us to think it might be a point between PI3K and Akt. PI3K phosphorylates PtdIns-4,5-P2 to yield PtdIns-3,4,5-P3. PtdIns-3,4,5-P3 in turn causes membrane localization of protein kinase B/Akt and the phosphoinositide-dependent kinase-1, which phosphorylates the Thr^{308} site (25). For maximal activation, however, the second site on Akt (Ser^{473}) must also be phosphorylated. The kinase regulating phosphorylation of Ser^{473} is not known, but several kinases, such as ILK-1 (26) and ATM (27), have been suggested.

The use of HPIs has been associated with direct effects on tumors, including those through modulation of the cell proteasome (reviewed in ref. 28). Ritonavir and saquinavir have both been shown to affect the 26S proteasome resulting in accumulation of p21 and IκB (20, 29). This effect of saquinavir has been reported previously to correlate with radiation sensitization (20). However, in our hands, ritonavir neither inhibited Akt phosphorylation nor resulted in radiation sensitization.

HPIs have been in clinical use since 1995 and are associated with side effects, including insulin resistance and diabetes (17). Because insulin signals through Akt (18, 19), we explored a possible link of HPIs to Akt inhibition. Three of the five HPIs we tested inhibited Akt phosphorylation and radiosensitized cells at pharmacologically achievable concentrations. Our data do not directly support the hypothesis that Akt inhibition is also the mechanism of insulin resistance. Of the two HPIs that did not reduce Akt phosphorylation and did not radiosensitize cells, indinavir is associated with a higher risk of developing diabetes than the other HPI (16, 30). It is likely that the insulin resistance associated with HPIs may be multifactorial (31, 32), although effects on Akt may play a role in some cases (33).

Table 6. Test of synergy for regrowth delay in time to reach tumor volume of 1,000 mm^3 in T24 xenografts ± amprenavir after radiation

Days to tumor volume of 1,000 mm^3 mean ± SD (range)			
Control (n = 5)	Amprenavir (n = 6)	6 Gy (n = 6)	6 Gy + Amprenavir (n = 5)
15.8 ± 3.2 (11-18)	13.2 ± 4.4 (7-18)	19.3 ± 2.1 (18-22)	30.8 ± 4.0 (26-35*)
Interaction term β (SE)		14.100 (3.006)	
Wald statistic		4.691	
Test of synergy (one-sided P)		<0.001	

*One animal did not reach a tumor volume of 1,000 mm^3 during observation period.

Table 7. Test of synergy for regrowth delay in time to reach tumor volume of 1,000 mm^3 in T24 xenografts ± nelfinavir after radiation

Days to tumor volume of 1,000 mm^3 mean ± SD (range)			
Control (n = 5)	Nelfinavir (n = 6)	6 Gy (n = 6)	6 Gy + Nelfinavir (n = 5)
15.8 ± 3.2 (11-18)	14.3 ± 3.1 (11-18)	19.3 ± 2.1 (18-22)	28.6 ± 7.1 (18-35*)
Interaction term β (SE)		10.733 (3.569)	
Wald statistic		3.007	
Test of synergy (one-sided P)		0.004	

*One animal did not reach a tumor volume of 1,000 mm^3 during observation period.

It nevertheless remains that three of the five HPIs tested resulted in down-regulation of Akt phosphorylation at Ser^{473} at clinically achievable concentrations. We tested two of the HPIs (amprenavir and nelfinavir) as adjuvant antitumor agents *in vivo* and saw synergistic sensitization with HPI and radiation. Because there is safety data on both amprenavir and nelfinavir for the last 5 years, they should be tested as radiation sensitizers in clinical trial.

Acknowledgments

Received 4/7/2005; revised 7/1/2005; accepted 7/7/2005.

Grant support: NIH grant 1 PO-1 CA75138 (W.G. McKenna) and GlaxoSmithKline research grant (A.K. Gupta).

The costs of publication of this article were defrayed in part by the payment of page charges. This article must therefore be hereby marked *advertisement* in accordance with 18 U.S.C. Section 1734 solely to indicate this fact.

We would like to thank Dr. A.V. Kachur for his assistance with high-performance liquid chromatography.

References

1. Perez CA, Brady LW, editors. Principles and practice of radiation oncology. 3rd ed. Philadelphia (PA): Lippincott; 1998.
2. Girinsky T, Lubin R, Pignon JP, et al. Predictive value of *in vitro* radiosensitivity parameters in head and neck cancers and cervical carcinomas: preliminary correlations with local control and overall survival. Int J Radiat Oncol Biol Phys 1993;25:147–8.
3. West CM, Davidson SE, Roberts SA, Hunter RD. Intrinsic radiosensitivity and prediction of patient response to radiotherapy for carcinoma of the cervix. Br J Cancer 1993;68:819–23.
4. Sheridan MT, O'Dwyer T, Seymour CB, Mothersill CE. Potential indicators of radiosensitivity in squamous cell carcinoma of the head and neck. Radiat Oncol Investig 1997;5:180–6.
5. Bonner JA, De Los Santos J, Waksal HW, Needle MN, Trummel HQ, Raisch KP. Epidermal growth factor receptor as a therapeutic target in head and neck cancer. Semin Radiat Oncol 2002;12:11–20.
6. O'Rourke DM, Kao GD, Singh N, et al. Conversion of a radioresistant phenotype to a more sensitive one by disabling erbB receptor signaling in human cancer cells. Proc Natl Acad Sci 1998;95:10842–7.
7. Sklar MD. The ras oncogenes increase the intrinsic resistance of NIH 3T3 cells to ionizing radiation. Science 1988;239:645–7.
8. McKenna WG, Weiss MC, Endlich B, et al. Synergistic effect of the v-*myc* oncogene with H-*ras* on radioresistance. Cancer Res 1990;50:97–102.
9. Rosser CJ, Tanaka M, Pisters LL, et al. Adenoviral-mediated PTEN transgene expression sensitizes Bcl-2-expressing prostate cancer cells to radiation. Cancer Gene Ther 2004;11:273–9.
10. Grana TM, Rusyn EV, Zhou H, Sartor CI, Cox AD. Ras mediates radioresistance through both phosphatidylinositol 3-kinase-dependent and Raf-dependent but mitogen-activated protein kinase/extracellular signal-regulated kinase kinase-independent signaling pathways. Cancer Res 2002;62:4142–50.
11. Gupta AK, Bakanauskas VJ, Cerniglia GJ, et al. The Ras radiation resistance pathway. Cancer Res 2001; 61:4278–82.
12. Gupta AK, McKenna WG, Weber CN, et al. Local recurrence in head and neck cancer: relationship to radiation resistance and signal transduction. Clin Cancer Res 2002;8:885–92.
13. Kim IA, Fernandes AT, Gupta AK, McKenna WG, Bernhard EJ. The influence of the Ras pathway signaling on tumor radiosensitivity. Cancer Metastasis Rev 2004; 23:227–36.
14. Gupta AK, Cerniglia GJ, Mick R, et al. Radiation sensitization of human cancer cells *in vivo* by inhibiting the activity of PI3K using LY294002. Int J Radiat Oncol Biol Phys 2003;56:846–53.
15. Deeks SG, Smith M, Holodniy M, Kahn JO. HIV-1 protease inhibitors. A review for clinicians. JAMA 1997; 277:145–53.
16. Carr A, Samaras K, Thorisdottir A, Kaufmann GR, Chisholm DJ, Cooper DA. Diagnosis, prediction and natural course of HIV-1 protease-inhibitor-associated lipodystrophy, hyperlipidaemia, and diabetes mellitus: a cohort study. Lancet 1999;353:2093–9.
17. Powderly WG. Long-term exposure to lifelong therapies. J Acquir Immune Defic Syndr 2002;29:S28–40.
18. Bae SS, Cho H, Mu J, Birnbaum MJ. Isoform-specific regulation of insulin-dependent glucose uptake by Akt/protein kinase B. J Biol Chem 2003;278:49530–6.
19. Cross DA, Watt PW, Shaw M, et al. Insulin activates protein kinase B, inhibits glycogen synthase kinase-3 and activates glycogen synthase by rapamycin-insensitive pathways in skeletal muscle and adipose tissue. FEBS Lett 1997;406:211–5.
20. Pajonk F, Himmelsbach J, Riess K, Sommer A, McBride WH. The human immunodeficiency virus (HIV)-1 protease inhibitor saquinavir inhibits proteasome function and causes apoptosis and radiosensitization in non-HIV-associated human cancer cells. Cancer Res 2002;62:5230–5.
21. Hu Q, Klippel A, Muslin AJ, Fantl WJ, Williams LT. Ras-dependent induction of cellular responses by constitutively active phosphatidylinositol-3 kinase. Science 1995;268:100–2.
22. Zhou BP, Hu MCT, Miller SA, et al. HER-2/*neu* blocks tumor necrosis factor induced apoptosis via the Akt/NF-κB pathway. J Biol Chem 2000;275:8027–31.
23. Carpenter CL, Cantley LC. Phophinositide kinases. Curr Opin Cell Biol 1996;8:153–8.
24. Thompson JE, Thompson CB. Putting the Rap on Akt. J Clin Oncol 2004;22:4217–26.
25. Kim S, Jee K, Kim D, Koh H, Chung J. Cyclic AMP inhibits Akt activity by blocking the membrane localization of PDK-1. J Biol Chem 2001;276:12864–70.
26. Persad S, Attwell S, Gray V, et al. Regulation of protein kinase B/Akt-serine-473 phosphorylation by integrin linked kinase (ILK): critical roles for kinase activity and amino acids arginine-211 and serine-343. J Biol Chem 2001;276:27462–9.
27. Viniegra JG, Martinez N, Modirassari P, et al. Full activation of PKB/Akt in response to insulin or ionizing radiation is mediated through ATM. J Biol Chem 2005;280:4029–36.
28. Sgadari C, Monini P, Barillari G, Ensoli B. Use of HIV protease inhibitors to block Kaposi's sarcoma and tumour growth. Lancet Oncol 2003;4:537–47.
29. Gaedicke S, Firat-Geier E, Constantiniu O, et al. Antitumor effect of the human immunodeficiency virus protease inhibitor ritonavir: induction of tumor-cell apoptosis associated with perturbation of proteasomal proteolysis. Cancer Res 2002;62:6901–8.
30. Noor MA, Seneviratne T, Aweeka FT, et al. Indinavir acutely inhibits insulin-stimulated glucose disposal in humans: a randomized, placebo-controlled study. AIDS 2002;16:F1–8.
31. Koster JC, Remedi MS, Qiu H, Nichols CG, Hruz PW. HIV protease inhibitors acutely impair glucose-stimulated insulin release. Diabetes 2003;52:1695–700.
32. Murata H, Hruz PW, Mueckler M. The mechanism of insulin resistance caused by HIV protease inhibitor therapy. J Biol Chem 2000;275:20251–4.
33. Ben-Romano R, Rudich A, Tirosh A, et al. Nelfinavir-induced insulin resistance is associated with impaired plasma membrane recruitment of the PI 3-kinase effectors Akt/PKB and PKC-ζ. Diabetologia 2004;47: 1107–17.

HIV Protease Inhibitors Block Akt Signaling and Radiosensitize Tumor Cells Both *In vitro* and *In vivo*

Anjali K. Gupta, George J. Cerniglia, Rosemarie Mick, et al.

Cancer Res 2005;65:8256-8265.